AIP | Applied Physics Letters

Ultrathin highly uniform Ni(Al) germanosilicide layer with modulated B8 type Ni5(SiGe)3 phase formed on strained Si1xGex layers

Linjie Liu, Lei Jin, Lars Knoll, Stephan Wirths, Alexander Nichau, Dan Buca, Gregor Mussler, Bernhard Holländer, Dawei Xu, Zeng Feng Di, Miao Zhang, Qing-Tai Zhao, and Siegfried Mantl

Citation: Applied Physics Letters **103**, 231909 (2013); doi: 10.1063/1.4838695
View online: http://dx.doi.org/10.1063/1.4838695
View Table of Contents: http://scitation.aip.org/content/aip/journal/apl/103/23?ver=pdfcov
Published by the AIP Publishing

Ultrathin highly uniform Ni(Al) germanosilicide layer with modulated B8 type $Ni_5(SiGe)_3$ phase formed on strained $Si_{1-x}Ge_x$ layers

Linjie Liu,[1,2,3] Lei Jin,[4] Lars Knoll,[1] Stephan Wirths,[1] Alexander Nichau,[1] Dan Buca,[1] Gregor Mussler,[1] Bernhard Holländer,[1] Dawei Xu,[1,2,3] Zeng Feng Di,[2] Miao Zhang,[2] Qing-Tai Zhao,[1,a)] and Siegfried Mantl[1]

[1]*Peter Grünberg Institute 9, Forschungszentrum Jülich, 52425 Jülich, Germany*
[2]*State Key Laboratory of Functional Material for Informatics, Shanghai Institute of Microsystem and Information Technology, CAS, Shanghai 200050, China*
[3]*University of Chinese Academy of Sciences, Beijing 100049, China*
[4]*Peter Grünberg Institute 5, Forschungszentrum Jülich, 52425 Jülich, Germany*

(Received 9 October 2013; accepted 15 November 2013; published online 5 December 2013)

We present a method to form ultrathin highly uniform Ni(Al) germanosilicide layers on compressively strained $Si_{1-x}Ge_x$ substrates and their structural characteristics. The uniform Ni(Al) germanosilicide film is formed with Ni/Al alloy at an optimized temperature of 400 °C with an optimized Al atomic content of 20 at. %. We find only two kinds of grains in the layer. Both grains show orthogonal relationship with modified B8 type phase. The growth plane is identified to be {10-10}-type plane. After germanosilicidation the strain in the rest $Si_{1-x}Ge_x$ layer is conserved, which provides a great advantage for device application. © *2013 AIP Publishing LLC*. [http://dx.doi.org/10.1063/1.4838695]

Strained silicon-germanium (SiGe) is a promising semiconductor material for nanoelectronics,[1–5] due to its high hole mobility and compatibility with existing Si technology.[6] Thin SiGe layer has been used as high hole mobility channel in p-type metal-oxide-semiconductor field effect transistors (MOSFETs).[7,8] Embedded SiGe at source/drain which creates uniaxial compressive strain in short Si channel p-MOSFETs has also been applied industrially to enhance the hole mobilities.[9] The band-gap engineering by tuning of the Ge content and the layer thickness also offers many applications for SiGe in optoelectronics, such as photodetectors,[10] modulators,[11] solar cells,[12] and quantum cascade lasers.[13] For all these applications, metal contacts on SiGe are very critical. Low resistivity contacts with homogeneous layers and smooth contact/SiGe interfaces are needed for device applications, especially nanometer devices[14] in order to reduce the resistance and minimize the device variability. In a Si based MOSFET Nickel (Ni) silicides are widely used at source/drain (S/D) for their advantages of low resistivity, low Si consumption, and simple process. In contrast, achieving homogeneous Ni germanosilicide (NiSiGe) layers with smooth interfaces is challenging due to Ge segregation, multi-phase formation, thermal agglomeration, and the elastic strain influence of the strained SiGe layer.[15–17] The morphology and thermal stability of germanosilicide on relaxed SiGe layers can be improved by incorporation of impurities, like carbon[18] or metal elements,[19,20] and using different annealing methods such as laser annealing[21] and microwave annealing.[22] However, formation of homogeneous germanosilicide layers on strained SiGe without strain relaxation, which has more potential use, is still a challenge.

In this work, we present a method to form homogeneous Ni Germanosilicide layers with low resistivity and smooth germanosilicide/SiGe interface on strained SiGe substrates. We identify a modulated B8 type phase of $Ni_5(SiGe)_3$ growing on strained SiGe layer.

Fully compressively strained 15 nm thick $Si_{0.64}Ge_{0.36}$ and 10 nm $Si_{0.55}Ge_{0.45}$ layers epitaxially grown by reduced pressure chemical vapor deposition (RPCVD) method[23] on Si (100) substrates were used. After cleaning and HF dip, the metal stack composed of multi Al/Ni layers was deposited by sputtering. The stack consists of 3 cycles of Al and Ni layers, starting with Al deposition. The total thickness of Ni was maintained at 5.7 nm, while the thickness of Al was varied by changing the deposition rate in order to adjust the atomic percentage of Al to 10 at. %, 20 at. %, and 30 at. % among the {Al/Ni} layers. The germanosilicidation was then triggered by forming gas annealing for 15 s at 300 °C, 400 °C, 500 °C, and 600 °C, respectively. The unreacted metal was subsequently etched in H_2SO_4 solution.

The germanosilicide layer structure and composition were investigated based on cross section transmission electron microscopy (XTEM) and Rutherford backscattering spectrometry (RBS) on samples formed with variable Al content. The morphology of the germanosilicide formed on $Si_{0.64}Ge_{0.36}$ after 400 °C annealing is shown in Figure 1. For 10% Al in the metal stack, the presence of Al at the SiGe surface does not differentiate the process from the case of pure Ni: A discontinuous germanosilicide layer with grains consuming the complete SiGe layer is observed (Figure 1(a)). By analogy, a SiGe-rich phase of $Ni_x(SiGe)_y$ with $x < y$ is most probably formed. The mediation role of Al in the Ni-SiGe reaction is seen for 20 at. % (Figure 1(b)) and 30 at. % Al (Figure 1(c)). The controlled germanosilicide reaction results in the formation of homogeneous germanosilicide layers with sharp interfaces to the left SiGe. For both cases 11 nm of germanosilicide is formed by consuming about 6.3 nm of the initial SiGe layer. Secondary ion mass spectrometry (SIMS) results as shown in the inset of Figure 1(b), indicate that Ni,

a)Author to whom correspondence should be addressed. Electronic mail: q.zhao@fz-juelich.de.

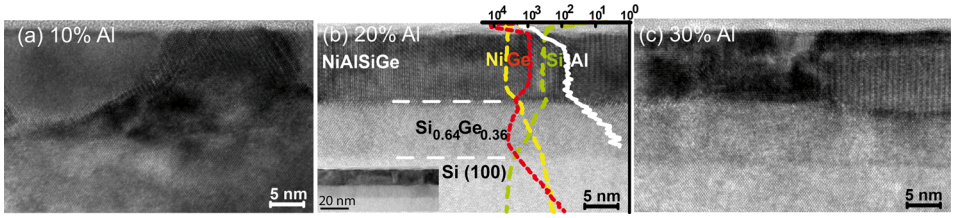

FIG. 1. TEM micrographs for germanosilicides formed with (a) 10% Al, (b) 20% Al, and (c) 30% Al on 20 nm $Si_{0.64}Ge_{0.36}$ at 400 °C. The layer formed with 20% Al shows the best layer quality with a homogenous layer thickness and very sharp germanosilide/SiGe interface. The SIMS distributions of Ni, Al, Ge, and Si atoms are shown in the inset of Figure 1(b). In Figure 1(b) the inset TEM image with low a magnification shows a very uniform germanosilicide layer in a large scale.

Al, Si, and Ge elements distribute homogeneously in the germanosilicide layer formed with 20% Al, which suggests an uniform phase distribution in the layer. The increase of the Al content to 30% does not change the thickness of the germanosililicide layer (Figure 1(c)). However, according to the TEM analyses, the highest crystal quality is obtained for 20 at. % Al (Figure 1(b)). The TEM image in the inset of Figure 1(b) further shows that the layer is very uniform in a large scale. For an Al percentage of 10%, the relatively thicker germanosilicide layer indicates strong Ni diffusion. For an Al percentage of 20%, the Al interface atoms and the larger Al thickness reduce the Ni amount arriving at the SiGe interface and facilitate controlled germanosilicide growth. Al is more favorable to bond with SiGe, balancing the Ni-Si and Ni-Ge reactions and suppressing Ge segregation and out-diffusion.[19] This is a precondition for homogeneous layer formation allowing uniform Ge incorporation into the thermodynamically favorable NiSi structure. The sheet resistance for a sample with 20 at. % Al was measured to be 43.6 Ω/sq, while that with 30 at. % Al is 50.6 Ω/sq, corresponding to a small specific resistivity of 48 μΩ cm and 55.7 μΩ cm, respectively.

While a germanosilicide layer with an Al content of 20 at. % seems to offer the best layer morphology, the formation temperature was investigated for this particular condition. Similar Ni-rich phase formation was observed by RBS for 300 °C and 400 °C formation temperatures, but the lowest channeling yield was found for 400 °C annealed samples (Figure 2), indicating higher crystal quality. The simulation of the RBS spectrum shows a composition of $Ni_5(Si_{0.64}Ge_{0.36})_3$ with a very little amount of Al in the layer. Raising the formation temperature to 500 °C, the Ni atoms diffuse deeper into the SiGe layer, seen by the lower and broader random Ni signal (Figure 2 inset). In conclusion, the germanosilicide phase transforms from Ni-rich to mono-germanosilicide by increasing the annealing temperature from 300 °C to 500 °C with the best crystalline quality for 400 °C annealing.

In the following, we focus our in-depth analyses on the 400 °C formed Ni-germanosilices with 20 at. % Al. Cross section and plan view high resolution TEM (HRTEM) were employed to get a better insight into the crystal structure. From the cross section results (Figure 3), it was found that the layer is not single-crystalline, but composed of two types of grains, denoted as "Grain A" and "Grain B." By careful

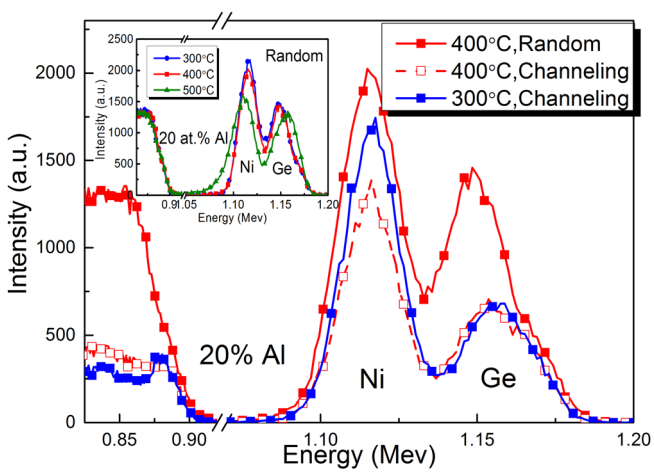

FIG. 2. Phase transition and layer quality analysis from RBS random and channeling measurements. Channeling comparison between germanosilicide layer formed at 300 °C and 400 °C indicates a better crystal quality formed at 400 °C. The inset shows Germanosilicide layers formed at different temperatures with 20 at. % Al, showing a phase transition from Ni rich phase at 300 °C to mono-germanosilicide phase at 500 °C by the RBS spectra.

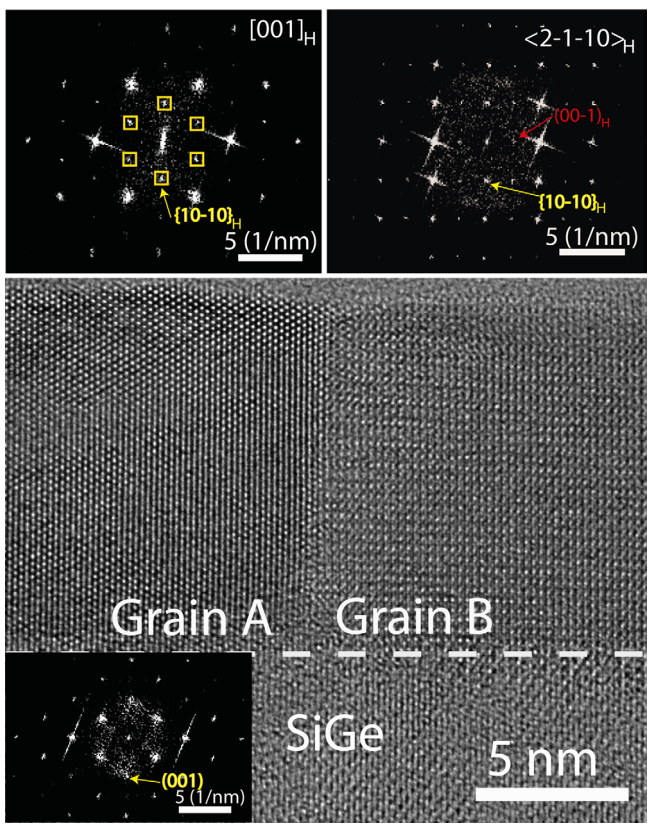

FIG. 3. X-HRTEM image for the layer formed with 20% Al at 400 °C. Two type of grains with modulated $Ni_5(SiGe)_3$ B8 phase and {10-10}-type growth plane are distinguished. Zone axes are [001] and ⟨2-110⟩, respectively, with orthogonal relationship.

analyses of all possible structures containing Ni, Al, Si, and Ge, the Fast Fourier transforms (FFT) shown in Figure 3 were indexed on the basis of a B8 type phase of $Ni_5(SiGe)_3$.[24] Though it has been reported that Ni_5Ge_3 possesses a monoclinic structure, we adopt the hexagonal B8 phase for description convenience. The transformation matrix between monoclinic and hexagonal lattices is given by

$$\begin{pmatrix} h \\ k \\ l \end{pmatrix}_{\mathrm{M}} = \begin{pmatrix} 3 & 3 & 0 \\ 1 & -1 & 0 \\ 1 & 1 & -1 \end{pmatrix} \begin{pmatrix} h \\ k \\ l \end{pmatrix}_{\mathrm{H}},$$

where $(hkl)_H$ and $(hkl)_M$ denote the Miller indexes in the hexagonal and monoclinic systems, respectively. It can be clearly seen from Figure 3 that both grain A and grain B possess a growth front of $\{10\text{-}10\}_H$ planes, which, in addition, have an orthogonal relationship.

The orthogonal relationship of the two domains is confirmed by plan-view HRTEM images and their corresponding FFT patterns shown in Figure 4. Two kinds of grains with a clear grain boundary can be recognized. Periodic atom planes distribute orthogonal to each other. The fact that there are only two kinds of highly ordered orthogonal grains with the same growth plane in the film, explains the low channeling yield observed by RBS, even when the film has a different crystalline structure compared to the substrate.

The B8 type $Ni_5(SiGe)_3$ phase was here also evidenced by the θ-2θ XRD scan and the pole figure measurements (inset Figure 5). The SiGe position of the XRD scan (inset Figure 5) demonstrates that the elastic strain in the unreacted SiGe layer is conserved after processing. This is further proved by the absence of misfit dislocations at the SiGe/Si substrate. Ni_5Ge_3 was found to form simultaneously with NiGe by Ni reaction with Ge.[25] It is surprising to show, in this paper, that a uniform $Ni_5(SiGe)_3$ layer with a low resistivity was formed on fully strained SiGe substrates.

The above presented results indicate 20 at. % Al and anneal at 400 °C as the optimum process for germanosilicidation of strained $Si_{0.64}Ge_{0.36}$ layers. This process was also

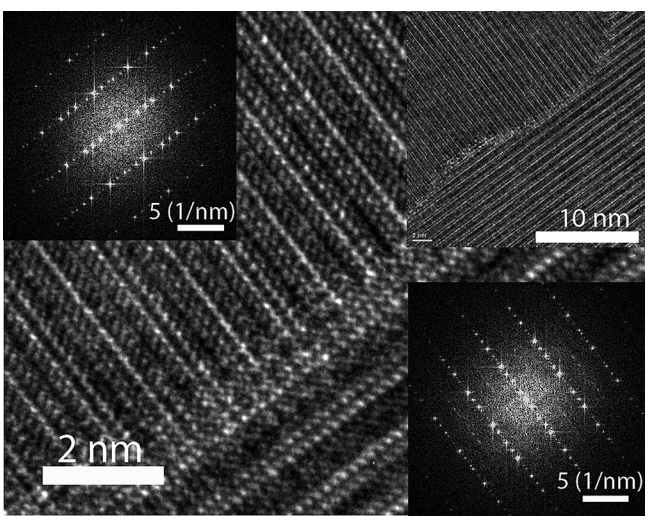

FIG. 4. Orthogonal relationship of the two grains is shown in the plan view HRTEM image. Their FFT diffraction patterns present the same orthogonal relationship (insets).

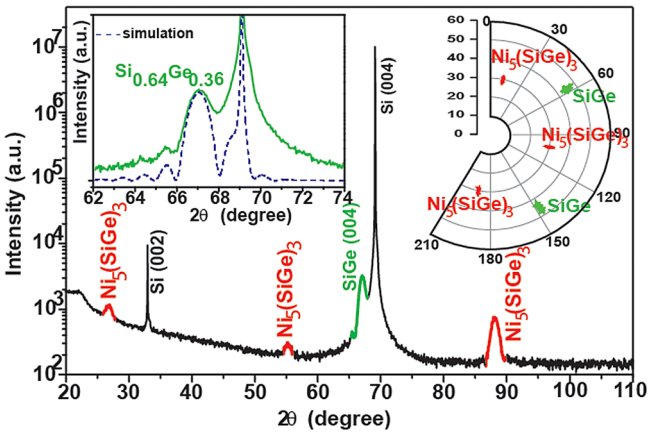

FIG. 5. XRD curve showing the main diffraction peaks of $Ni_5(SiGe)_3$. The 3 $Ni_5(SiGe)_3$ peaks correspond to {10-10} plane in the B8 phase. The inset shows magnified SiGe (004) reflections as evidence of fully strained status of the unconsumed SiGe layer. The pole figure completes the XRD analyses with clear evidence of $Ni_5(SiGe)_3$ B8 phase with a $\{10\text{-}10\}_H$ growth plane through the $(11\text{-}20)_H$ reflection. The Si related peaks are (022) reflections, [001] orientation.

applied to strained $Si_{0.55}Ge_{0.45}$ layer which presents a larger built-in elastic strain of about 1.9%. An 11 nm layer with high crystalline quality, a smooth surface and an abrupt interface to the 3.7 nm remained $Si_{0.55}Ge_{0.45}$ layer was formed (not shown). We assume that the Al mediated epitaxial growth of quaternary silicides is independent on the Ge contents and incorporated elastic strain in the investigated range from 36% to 45% Ge, corresponding to 1.5% and 1.9% compressive strain. Since the in-plane lattice constant of the SiGe layer does not change with the Ge content, we assume that the B8 type $Ni_5(SiGe)_3$ phase has a preferential $\{10\text{-}10\}_H$ growth planes due to the better lattice match with SiGe. The growth mechanism is still not very clear, which will be further investigated.

In summary, we have demonstrated homogeneous Ni(Al) germanosilicide formation if 20% Al is contained in the metal layer after subsequent annealing at 400 °C. HRTEM analysis identified only two kinds of grains in the film. Both grains have modified B8 type phase, and the growth plane is {10-10}-type plane. The zone axes of the grains have orthogonal relationship. Al mediation is experimentally proved to promote the growth of very thin homogeneous quaternary silicides on SiGe layers with Ge content up to 45 at. % and compressive strain up to 1.9%, providing a method for advanced contacts on strained SiGe for both electrical and optical nanometer devices.

This work was performed at the Peter Grünberg Institut-9, Forschungszentrum Jülich and was partially supported by the European project "Places2Be" and CAS International Collaboration and Innovation Program on High Mobility Materials Engineering. Linjie Liu and Dawei Xu thank China Scholarship Council (CSC) for the financial support.

[1]J. Nah, D. C. Dillen, K. M. Varahramyan, S. K. Banerjee, and E. Tutuc, Nano Lett. **12**, 108 (2012).
[2]E. K. Lee, L. Yin, Y. Lee, J. W. Lee, S. J. Lee, J. Lee, S. N. Cha, D. Whang, G. S. Hwang, K. Hippalgaonkar, A. Majumdar, C. Yu, B. L. Choi, J. M. Kim, and K. Kim, Nano Lett. **12**, 2918 (2012).
[3]S. T. Le, P. Jannaty, X. Luo, A. Zaslavsky, D. E. Perea, S. A. Dayeh, and S. T. Picraux, Nano Lett. **12**, 5850 (2012).
[4]M. B. Ishai and F. Patolsky, J. Am. Chem. Soc. **131**, 3679 (2009).

[5]G. Joshi, H. Lee, Y. Lan, X. Wang, G. Zhu, D. Wang, R. W. Gould, D. C. Cuff, M. Y. Tang, M. S. Dresselhaus, G. Chen, and Z. Ren, Nano Lett. **8**, 4670 (2008).
[6]M. V. Fischetti and S. E. Laux, J. Appl. Phys. **80**, 2234 (1996).
[7]W. Yu, B. Zhang, Q. T. Zhao, D. Buca, J. Hartmann, R. Luptak, G. Mussler, A. Fox, K. K. Bourdelle, X. Wang, and S. Mantl, IEEE Electron Device Lett. **33**, 758 (2012).
[8]R. A. Minamisawa, M. Schmidt, L. Knoll, D. Buca, Q. T. Zhao, J. M. Hartmann, K. K. Bourdelle, and S. Mantl, IEEE Electron Device Lett. **33**, 1105 (2012).
[9]M. L. Lee, E. A. Fitzgerald, M. T. Bulsara, M. T. Currie, and A. Lochtefeld, J. Appl. Phys. **97**, 011101 (2005).
[10]D. Buca, S. Winnerl, S. Lenk, C. Buchal, and D. X. Xu, Appl. Phys. Lett. **80**, 4172 (2002).
[11]P. Chaisakul, D. Marris-Morini, M.-S. Rouifed, G. Isella, D. Chrastina, J. Frigerio, X. Le Roux, S. Edmond, J.-R. Coudevylle, and L. Vivien, Opt. Express **20**, 3219 (2012).
[12]C. Pan, Z. Luo, C. Xu, J. Luo, R. Liang, G. Zhu, W. Wu, W. Guo, X. Yan, J. Xu, Z. L. Wang, and J. Zhu, ACS Nano **5**, 6629 (2011).
[13]P. Sookchoo, F. F. Sudradjat, A. M. Kiefer, H. Durmaz, R. Paiella, and M. G. Lagally, ACS Nano **7**, 2326 (2013).
[14]S. E. Thompson and S. Parthasarathy, Mater. Today **9**, 20 (2006).
[15]J. Seger, T. Jarmar, Z.-B. Zhang, H. H. Radamson, F. Ericson, U. Smith, and S.-L. Zhang, J. Appl. Phys. **96**, 1919 (2004).
[16]K. L. Pey, W. K. Choi, S. Chattopadhyay, H. B. Zhao, E. A. Fitzgerald, D. A. Antoniadis, and P. S. Lee, J. Vac. Sci. Technol. A **20**, 1903 (2002).
[17]Q. T. Zhao, D. Buca, S. Lenk, R. Loo, M. Caymax, and S. Mantl, Microelectron. Eng. **76**, 285 (2004).
[18]B. Zhang, W. Yu, Q. T. Zhao, D. Buca, B. Hollander, J. M. Hartmann, M. Zhang, X. Wang, and S. Mantl, Electrochem. Solid-State Lett. **14**, H261 (2011).
[19]B. Zhang, W. Yu, Q. T. Zhao, G. Mussler, L. Jin, D. Buca, B. Hollander, J. M. Hartmann, M. Zhang, X. Wang, and S. Mantl, Appl. Phys. Lett. **98**, 252101 (2011).
[20]Y.-J. Xu, G.-P. Ru, Y.-L. Jiang, X.-P. Qu, and B.-Z. Li, Appl. Surf. Sci. **256**, 305 (2009).
[21]Y. Setiawan, P. S. Lee, K. L. Pey, X. C. Wang, G. C. Lim, and B. L. Tan, Appl. Phys. Lett. **90**, 073108 (2007).
[22]C. Hu, P. Xu, C. Fu, Z. Zhu, X. Gao, A. Jamshidi, M. Noroozi, H. Radamson, D. Wu, and S.-L. Zhang, Appl. Phys. Lett. **101**, 092101 (2012).
[23]S. Wirths, D. Buca, A. T. Tiedemann, P. Bernardy, B. Holländer, T. Stoica, G. Mussler, U. Breuer, and S. Mantl, Solid-State Electron. **83**, 2 (2013).
[24]A. K. Larsson and R. Withers, J. Alloys Compd. **264**, 125 (1998).
[25]F. Nemouchi, D. Mangelinck, C. Bergman, G. Clugnet, P. Gas, and J. L. Lábár, Appl. Phys. Lett. **89**, 131920 (2006).